Kent Academic Repository

Chisty, Liisa T, Toseland, Christopher P., Fili, Natalia, Mashanov, Gregory I, Dillingham, Mark S, Molloy, Justin E and Webb, Martin R (2013) *Monomeric PcrA helicase processively unwinds plasmid lengths of DNA in the presence of the initiator protein RepD.* Nucleic acids research, 41 (9). pp. 5010-5023. ISSN 1362-4962.

Monomeric PcrA helicase processively unwinds plasmid lengths of DNA in the presence of the initiator protein RepD

Liisa T. Chisty[1], Christopher P. Toseland[1,2], Natalia Fili[1,2], Gregory I. Mashanov[1], Mark S. Dillingham[3], Justin E. Molloy[1] and Martin R. Webb[1,*]

[1]MRC National Institute for Medical Research, Mill Hill, London NW7 1AA, UK, [2]Institut für Zelluläre Physiologie and Center for NanoScience (CeNS), Physiologisches Institut, Ludwig Maximilians Universität, Munich 80336, Germany and [3]DNA-protein Interactions Unit, School of Biochemistry, Medical Sciences Building, University of Bristol, University Walk, Bristol BS8 1TD, UK

ABSTRACT

The helicase PcrA unwinds DNA during asymmetric replication of plasmids, acting with an initiator protein, in our case RepD. Detailed kinetics of PcrA activity were measured using bulk solution and a single-molecule imaging technique to investigate the oligomeric state of the active helicase complex, its processivity and the mechanism of unwinding. By tethering either DNA or PcrA to a microscope coverslip surface, unwinding of both linear and natural circular plasmid DNA by PcrA/RepD was followed in real-time using total internal reflection fluorescence microscopy. Visualization was achieved using a fluorescent single-stranded DNA-binding protein. The single-molecule data show that PcrA, in combination with RepD, can unwind plasmid lengths of DNA in a single run, and that PcrA is active as a monomer. Although the average rate of unwinding was similar in single-molecule and bulk solution assays, the single-molecule experiments revealed a wide distribution of unwinding speeds by different molecules. The average rate of unwinding was several-fold slower than the PcrA translocation rate on single-stranded DNA, suggesting that DNA unwinding may proceed via a partially passive mechanism. However, the fastest dsDNA unwinding rates measured in the single-molecule unwinding assays approached the PcrA translocation speed measured on ssDNA.

INTRODUCTION

DNA helicases are involved in many aspects of DNA metabolism, acting as monomer, homo-oligomer or heteromeric complex. These motor proteins are grouped into superfamilies based on conserved amino acid sequences and, more recently, on other properties as well (1,2). Some of the best characterized helicases belong to superfamily 1, including *Escherichia coli* Rep and UvrD and *Bacillus stearothermophilus* PcrA, which share considerable structural similarity. Rep is involved in movement of the replisome on genomic DNA (3). Monomers of Rep translocate single-stranded DNA (ssDNA) in a 3′–5′ manner; however, dimerization is required for helicase activity (4). UvrD has multiple roles in DNA repair (5,6). Similar to Rep, UvrD has been shown to translocate single-stranded DNA (ssDNA) as a monomer, but it is suggested that oligomerization is required for helicase activity. The helicase activity of these two proteins is also enhanced by additional proteins, such as MutL and the ϕX174 bacteriophage cisA protein in the cases of UvrD and Rep, respectively (7–9).

PcrA is an essential helicase in many bacteria with a role in genomic DNA repair and in asymmetric rolling-circle plasmid replication (10). On its own, PcrA has difficulty separating even short lengths of double-stranded DNA (dsDNA) (11,12). However, its rate and processivity of unwinding are greatly enhanced by the plasmid-encoded replication initiation protein (11,13,14). The initiator protein used in this study is RepD, which binds a specific DNA sequence known as the double-stranded origin of replication (DSO) on the plasmid, termed *ori*D.

*To whom correspondence should be addressed. Tel: +44 2088 162078; Fax: +44 2089 064477; Email: mwebb@nimr.mrc.ac.uk

The authors wish it to be known that, in their opinion, the first three authors should be regarded as joint First Authors.

RepD nicks one DNA strand rapidly, and this enables PcrA to load onto the short length of exposed ssDNA (15,16). In the presence of ATP, PcrA then moves along one DNA strand (in the 3′–5′-direction) and unwinds the plasmid substrate, liberating a nascent single-stranded piece of DNA. Replication of the DNA strand along which PcrA travels is accomplished by DNA polymerase III. Once the plasmid is fully unwound and one strand fully replicated, the process is terminated at the newly formed *ori*D. The other strand, which has its own single-strand origin of replication site, is replicated by DNA polymerase I. *In vivo* the nascent single-strand is decorated with a protein called ssDNA-binding protein (SSB), which protects it from degradation. In the experiments reported here, we do not include the DNA polymerase enzymes; therefore, both ssDNA products can bind SSB.

Several crystal structures have led to a structural model of how a monomer of PcrA could move along DNA in a 3′–5′-direction by changes in a series of base-binding pockets across the protein (17–19). Kinetic measurements have shown that it hydrolyzes one ATP molecule per base moved, both in ssDNA translocation and dsDNA separation (14,20,21). However, the active oligomeric state of PcrA has not been unequivocally identified. Some kinetic experiments indicate that PcrA must form a dimer to unwind dsDNA (22). However, based on work with other helicases, an alternative model suggests that multiple monomers might align on a stretch of DNA to bring about unwinding (23). For plasmid unwinding (*in vivo*), accessory proteins, such as RepD, are required for PcrA to unwind DNA, and questions remain as to the oligomeric state of active PcrA and its processivity in this context.

Another fundamental question concerning the PcrA helicase mechanism is how its ability to separate, or unwind, the two complementary strands of dsDNA is coupled to its ability to translocate along the ssDNA backbone. In other words, its activities when moving along dsDNA compared with those when it moves along ssDNA. Such comparisons have been proposed (24) as a way to determine to what extent unwinding is an active process or a passive 'by-product' of the translocation mechanism (25). After this concept, in an *active* mechanism, helicase movement forces the two strands apart, for example, using a wedge domain coupled to ATP hydrolysis that produces a combination of force and movement. In a *passive* mechanism, thermal fluctuations in the degree of pairing at the end of the dsDNA allow the helicase to translocate; hence, the helicase must await fortuitous separation, which may slow its progress. Hence, helicases that have similar rates of movement on dsDNA and ssDNA are considered active, whereas those with slower translocation rates on dsDNA than ssDNA are termed *passive*. In practice, it would be expected that a range of intermediate levels is also likely. An example of a helicase that might be considered optimally active is Dda (26).

In the current study, we have used a single-molecule assay, previously described for use with another helicase, AddAB (27,28), to visualize DNA unwinding by PcrA in real-time, monitoring the accumulation of fluorescently
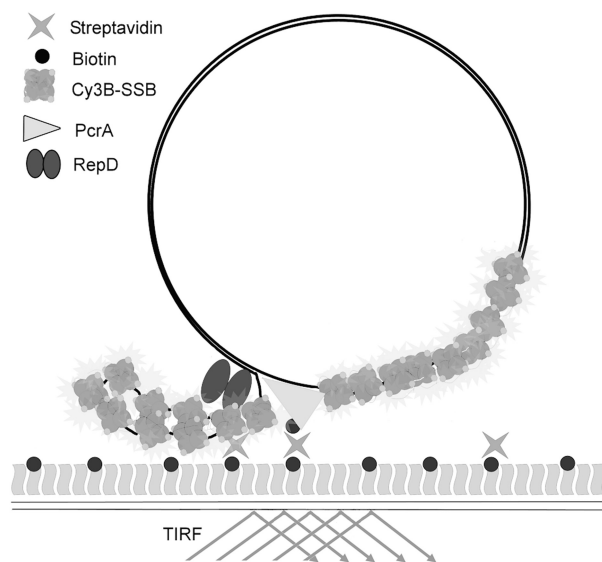
Figure 1. Cartoon of TIRFM assay for PcrA·RepD unwinding dsDNA. The figure represents a partially unwound plasmid with bioPcrA attached to a PEGylated surface, with the fluorescence excitation coming from below. It illustrates that the furthest distance the DNA can reach from the surface attachment is equivalent to half the plasmid length.

labeled SSB on the unwound ssDNA. SSB from *E. coli* was labeled with Cy3B to give an adduct Cy3B-SSB. Briefly, either linear dsDNA fragments or whole-circular plasmids, containing *ori*D, were first nicked by the initiator protein RepD and then allowed to interact with PcrA. Using biotinylation, the active complex was immobilized onto a streptavidin-coated microscope coverslip and visualized by TIRFM (total internal reflection fluorescence microscopy) (Figure 1). Two experimental geometries were adopted, in which either the dsDNA template or the helicase were surface immobilized, so that evolution of the ssDNA product occurred in a fixed position within the evanescent field of the TIRF imaging system. ATP-driven unwinding of the dsDNA substrates was then followed in real time by the appearance of fluorescent spots of gradually increasing intensity. By immobilizing either PcrA or the DNA, this experimental approach allowed comparison of the activity of PcrA free in solution with that of individually immobilized helicases. The previous work showed that the immobilization procedure had little or no effect on the average rate of unwinding for another helicase, AddAB, and indicated that would also be so for RecBCD (27,29). The assay gave a direct measurement of individual helicase unwinding activity on individual dsDNA molecules, without use of intercalating or other DNA labels, which may perturb the helicase unwinding activity. To complement the single-molecule assays, we also performed conventional bulk assays using a coumarin-labeled SSB (DCC-SSB), which gives a large fluorescence increase on binding ssDNA, allowing dsDNA unwinding to be measured by stopped-flow methods. We also compared the rate of dsDNA plasmid unwinding with the rate of PcrA translocation on ssDNA, using a coumarin-labeled PcrA that gives a signal on arrival at the end of the ssDNA template.

Results from the current work provide, for the first time, strong evidence that a single-PcrA monomer in the presence of RepD can unwind dsDNA processively. The data also provide information about the heterogeneity of PcrA activity, its processivity and its interaction with RepD. The data suggest a partially passive mechanism of unwinding, whereby at physiological ATP concentrations, some PcrA·RepD complexes are able to unwind dsDNA at similar speeds to the ssDNA translocation rate (24,25), but the majority unwind at a rate several times slower.

MATERIALS AND METHODS

Materials

Cy3B-maleimide was from GE Healthcare; IDCC (*N*-[2-(iodoacetamido)ethyl]-7-diethylaminocoumarin-3-carboxamide) and MDCC (*N*-[2-(1-maleimidyl)ethyl]-7-diethylaminocoumarin-3-carboxamide) were synthesized by Dr J. E. T. Corrie (NIMR, UK) (30). All oligonucleotides were purchased from Eurogentec Ltd, UK. All other chemicals and reagents were obtained from Sigma-Aldrich (Gillingham, UK), unless noted in the text. Plasmid substrates were prepared as described (14). Cy3B-SSB (27), DCC-SSB (31,32) and MDCC-PBP (33,34) were prepared and characterized, essentially as previously described. *B. stearothermophilus* PcrA (35) and *Staphylococcus aureus* RepD (14,36) were prepared as described previously, but they were purified by gel filtration.

BioPcrA (Biotag-PcrA) was expressed from pET22b vector containing full-length wild-type PcrA with a 20 amino acid tag at the N-terminus (MSG LND IFE AQK IEW HEG GG). The lysine is the target for *in vivo* biotinylation by the *E. coli* BirA enzyme. BL21 (DE3) cells (Novagen) were transformed with the modified plasmid, pET22bpcrA, and pBirACm (Avidity) and grown to mid-log phase at 37°C in L broth, supplemented with the appropriate antibiotics. Isopropyl β-D-1-thiogalactopyranoside (IPTG) and biotin were added to 1 mM and 50 μM, respectively, and the cells were grown for a further 3 h at 37°C. Cells were sonicated, and ammonium sulfate (50% saturation v/v) was added to the soluble extract. The precipitated material was recovered, and biotinylated proteins were isolated by affinity chromatography using Softlink Avidin resin (Promega), according to the manufacturer's instructions. HiTrap heparin chromatography (GE Healthcare), dialysis, storage and quantification of bioPcrA were then carried out essentially as described previously for the native protein (35).

Cy3B-bioPcrA and MDCC-PcrA were prepared by labeling (E449C)bioPcrA with Cy3B-maleimide and (K138C)PcrA with MDCC, respectively. (E449C)BioPcrA was prepared by creating the cysteine mutation at E449, a surface residue on bioPcrA, using QuikChange site-directed mutagenesis kit (Agilent) according to manufacturer's instructions with a primer pair (TCG GCG AGC TAT GTA TGA TCG GGC TTG GCG CCA and AGC CCG ATC ATA CAT AGC TCG CCG AGC GCC TCA AA). The protein was then prepared as described earlier in the text. Before labeling, dithiothreitol (DTT) was removed from (E449C)bioPcrA using PD-10 column (GE healthcare) in 50 mM Tris–HCl, pH 7.5, 300 mM NaCl and 3 mM MgCl₂. The (E449C)bioPcrA was labeled with 2-fold excess of Cy3B-maleimide for 1 h at room temperature in the same buffer. Free fluorophore was removed by elution through a PD-10 column, and the labeled protein was stored similarly to unlabeled protein. MDCC-PcrA(K138C) was produced by same method of site-directed mutagenesis with primers ATA GAC CCG AAA TGT TTT GAG CCG CGG ACG ATT TTA and TCC GCG GCT CAA AAC ATT TCG GGT CTA TGT TTT TTT. Expression and purification were done as for wild-type protein. Labeling with MDCC and purification of the labeled product was done similarly to Cy3B-bioPcrA.

Different lengths of linear DNA substrates were generated by PCR using the hot start Phusion polymerase (New England Biolabs), as described previously based on the pCER*ori*D (14,27). Using a single–5′-biotin–triethyleneglycol forward primer and various non-biotinylated reverse primers, 5′-biotinylated linear fragments of different lengths were also produced. Using this design, the *ori*D sequence is positioned at the opposite end of the dsDNA template to the biotin moiety. Non-biotinylated fragments were generated in the same way for studying the activity of immobilized bioPcrA. All PCR products were analyzed by agarose gel electrophoresis and purified by gel extraction and ethanol precipitation. Circular plasmid substrates were prepared as described previously (14).

Experimental solutions

Except where mentioned in the text, all experiments were performed at 23°C, and the buffers used were TB buffer = 10 mM NaCl, 25 mM Tris–HCl, pH 7.5; TP buffer = 100 mM KCl, 10 mM MgCl₂, 1 mM EDTA and 50 mM Tris–HCl, pH 7.5.

Stopped-flow measurements

Stopped-flow experiments were carried out using a HiTech SHU-61SX2 stopped-flow fluorimeter (TgK scientific Ltd) with a mercury–xenon light source (excitation 436 nm; emission 455 nm cut-off filter of Schott glass) and Kinetic Studio 2 software (TgK Scientific Ltd).

dsDNA unwinding in bulk solution was measured using DCC-SSB. RepD was incubated with non-biotinylated DNA for 10 min at 30°C to form the covalent RepD–DNA complex; then PcrA was incubated with this RepD–DNA complex for 2 min. The unwinding was initiated by rapid mixing with ATP in the stopped-flow apparatus. Final conditions after mixing were 0.5 nM DNA of various lengths, 100 nM PcrA, 2 nM RepD, 200 nM DCC-SSB tetramers and 1 mM ATP (in TP buffer). Theoretical curves were fitted to the data using both the Kinetic studio 2 software, and Grafit (37). Generally, fitting was performed on the average of at least three acquisitions, and data were obtained from two separate measurements.

For measurement of ssDNA translocation, 100 nM MDCC-PcrA was pre-mixed with 1 μM oligo(dT) of

various lengths, then rapidly mixed in the stopped-flow fluorimeter with 200 µM ATP (in TP buffer). All concentrations are those in the mixing chamber. Fluorescence was followed with time, and the average of three measurements was fitted with Grafit (37).

Steady-state ATPase measurements

This assay was used to confirm the full activity of labeled PcrA variants. Fluorescence was measured using a Cary Eclipse fluorometer with a xenon light source. Steady-state ATPase measurements were measured in TP buffer (60 µl) at 20°C, containing 2 nM PcrA, or bioPcrA, 500 nM dT_{20} and 10 µM phosphate biosensor, MDCC-PBP, with varying ATP concentrations as substrate. ATPase activity was measured by the change in fluorescence observed as MDCC-PBP bound the phosphate product. Linear fits to the start of the curves were performed before fitting these rates to the Michaelis–Menten kinetic model using Grafit software (37).

Size-exclusion chromatography and multi-angle light scattering

The oligomeric states of wild-type PcrA and bioPcrA were determined using a JASCO PU-1580 HPLC connected to Optilab Rex (Wyatt) light scattering detector and a differential refractometer (Dawn Helios from Wyatt). The protein was chromatographed using Superdex 200 HR 10/30 column (GE Healthcare) in TP buffer at a flow rate of 0.5 ml min^{-1}. Hundred-microliter samples were injected at a concentration of 0.5 mg ml^{-1}. A refractive index increment was set to value of 0.185 ml mg^{-1}. The data were recorded using a JASCO Chrompass Chromatography data system and ASTRA software.

TIRF imaging

Single-molecule imaging was performed using a custom-built, objective-coupled TIRFM apparatus, as previously described (28,38). TIRF excitation was provided by a 532 nm, 50 mW, solid-state laser (Suwtech 532-50 with 1500 LDC controller, SP3-Plus), and the emitted fluorescence was imaged onto an electron-multiplying charge-coupled device (EMCCD, iXon897BV, Andor). Using a neutral density filter OD = 1, the final laser power at the surface was ~2 µW µm^{-2}. Images were acquired at 20 Hz. For time-lapse imaging, the laser was activated for 50 ms, synchronized to the camera and frame acquisition occurred at variable intervals (up to many seconds), until the next camera frame was acquired.

Single-molecule helicase assays

Surface chemistry and flow-cell construction was performed as described previously (27). Use of a polyethylene-glycol-(PEG)–coated ('PEGylated') surface minimized non-specific adsorption of the assay components.

To study DNA unwinding using surface-immobilized dsDNA, the PEGylated surface of the flow cell was treated for 15 min with 20 µg ml^{-1} streptavidin in TB buffer and then incubated for 30 min with biotinylated dsDNA (500 pM molecules) in TB buffer. After each step, excess unbound protein, or DNA, was washed out with TB buffer. The immobilized DNA was incubated with 500 nM RepD in TP buffer for 15 min at 30°C to yield the covalent RepD–DNA complex. PcrA (500 nM) was then added and allowed to bind for 5 min. The unwinding was initiated with 1 mM ATP in TP buffer, supplemented with 25 nM Cy3B-SSB. Buffer conditions and Cy3B-SSB concentration were chosen to ensure that binding occurs rapidly and at the stoichiometry of ~65 bases per SSB tetramer.

For surface-immobilized PcrA with linear DNA, the streptavidin-coated surface was first treated with 1 nM bioPcrA in TP buffer for 30 min and excess protein was washed out as above. 500 nM RepD was incubated with 16 nM non-biotinylated DNA for 10 min at 30°C to form the RepD–DNA complex. This complex was then added to the surface on which bioPcrA was immobilized. After 10 min incubation at room temperature, excess RepD–DNA was washed out. The unwinding measurement was initiated as previously described.

Plasmid DNA unwinding was measured similarly, except for the following differences. Most measurements used Cy3B-PcrA, to aid spot focusing before initiation of unwinding. In all, 8 nM plasmid was incubated with 250 nM RepD to form the RepD–plasmid complex, and time-lapse imaging was used to minimize the effect of photobleaching.

All experiments were performed at 22°C–24°C in the presence of an oxygen-scavenger system, consisting of 10 mg ml^{-1} glucose, 50 µg ml^{-1} glucose oxidase, 400 µg ml^{-1} catalase, 500 µg ml^{-1} bovine serum albumin, 1 mM DTT, 1 mM ascorbic acid and 1 mM methyl viologen. An ATP-regeneration system, consisting of 100 µg ml^{-1} creatine phosphokinase and 2.4 mM creatine phosphate, was also added to TP buffer.

Data analysis

Image analysis was performed using custom-written computer software (freely available at http://www.nimr. mrc.ac.uk/gmimpro/). Individual fluorescent spots were identified by a pattern-matching algorithm, and the putative target spots were then screened to eliminate those with constant, or instantaneously, increasing fluorescence. To identify and characterize the pauses and unwinding phases, a custom-written PERL algorithm (ActiveState Software Inc.) was used as described previously (27). For data smoothing, a window size of 21 points (i.e. spot intensity data measured from 21 consecutive video frames) was chosen after optimization, but the analysis was also performed with a window size of 11 points, in case excess smoothing occurred. The method (39) was modified to detect pauses using a running Student's *t*-test over a 21 point and 11 point window.

For experiments using circular plasmid dsDNA, fluorescent spots of gradually increasing intensity were detected as described earlier in the text for data obtained using linear dsDNA. Then the duration and amplitude of each unwinding event were determined automatically using Igor Pro software (WaveMetrics Inc). The initial rising

phase of fluorescence intensity was fitted to a single rising exponential function, and the event duration was defined as complete within 4 half-times (∼95%). Histograms of amplitude and duration distributions were fitted using Grafit (37).

RESULTS

Oligomeric state of biotinylated PcrA and wild-type PcrA using size-exclusion chromatography and multi-angle light scattering

The oligomeric state of bioPcrA and wild-type PcrA, in the absence of DNA, was assessed by size-exclusion chromatography-multi-angle light scattering (SEC-MALS, Supplementary Figure S1). Results showed that both proteins had the particle mass expected of the monomer. Thus, the bioPcrA is monomeric before surface immobilization (in the single-molecule experiments described later in the text), and both bioPcrA and native PcrA are monomeric before interacting with dsDNA substrates, in bulk and single-molecule assays.

Unwinding activity of bioPcrA and PcrA measured using bulk methods

Unwinding activity of biotinylated PcrA (bioPcrA) was characterized by ensemble, stopped-flow measurements and results were compared with the wild-type protein (14,31). Plasmid DNA was pre-equilibrated with RepD, mixed with bioPcrA, and unwinding was initiated by rapid mixing with 1 mM ATP. The unwinding time course was determined from the increase in fluorescence of DCC-SSB (see 'Materials and Methods' section). The experiment was repeated with various lengths of plasmid DNA.

Fluorescence records exhibited a lag phase followed by a linear increase in fluorescence until a break point to a slower increase in fluorescence (Supplementary Figure S2A). The lag phase, observed previously, may be due to initiation events at the DSO, *ori*D under the conditions of the bulk experiment, although its origins are not clear. We interpret the linear increase because of helicase unwinding and the final phase because of rearrangements of DCC-SSB on the ssDNA product. Duration of the unwinding phase increased linearly with plasmid length (Supplementary Figure S2B), consistent with complete unwinding of the DNA substrates. A linear fit to the average duration of the unwinding phase plotted against dsDNA template length gave a slope of 27 ($\pm$2) bp s^{-1}, which represents an unwinding rate similar to that of wild-type PcrA, 30 bp s^{-1} (14), suggesting that biotinylation of PcrA had little, if any, effect on its helicase activity.

Translocation rate of PcrA on ssDNA measured using bulk methods

Short lengths of ssDNA were used with the fluorescent MDCC-PcrA providing an endpoint signal. This labeled protein had activity identical to wild-type PcrA in plasmid unwinding assays. The fluorescence signal of MDCC-PcrA is high when completely bound within
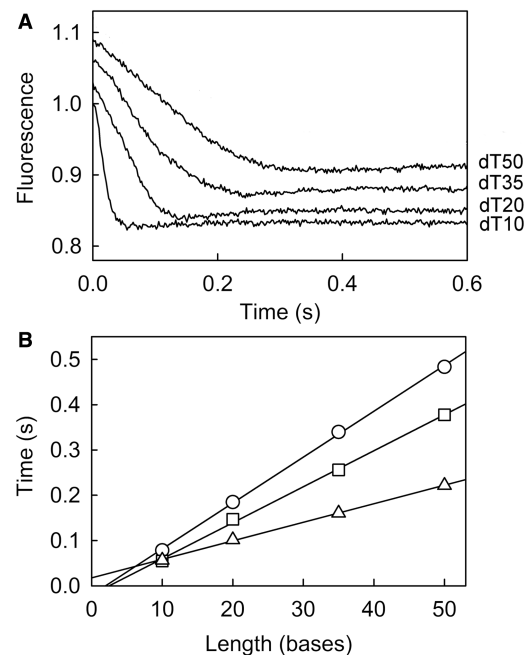
Figure 2. Translocation of MDCC-PcrA along ssDNA. (**A**) MDCC-PcrA was premixed with different lengths of oligo(dT), then rapidly mixed with ATP in the solution conditions (buffer and temperature, 22°C) of the TIRF measurements. The time to minimum fluorescence for each length represents the time for the last PcrA molecules to translocate to the 5′-end. The curves are offset from each other for clarity. (**B**) These time were plotted against length (squares) to give the translocation rate of 125 ($\pm$2) bases s^{-1} from the gradient. These plots are also shown for measurements under the conditions used by Dillingham *et al.* (21) for translocation (circles, 20°C, 50 mM Tris–HCl, pH 7.5, 150 mM KCl and 3 mM MgCl$_2$), giving 99 ($\pm$2) bases s^{-1}, and the solution plasmid unwinding conditions of Slatter *et al.* (14) (triangles, 30°C, 50 mM Tris–HCl, pH 7.5, 100 mM KCl, 10 mM MgCl$_2$ and 1 mM EDTA), giving 244 ($\pm$4) bases s^{-1}.

ssDNA (i.e. in the middle) and low when bound at the end. This was demonstrated by binding MDCC-PcrA to different lengths of oligo(dT), using rapid-mixing stopped-flow and following fluorescence with time (Supplementary Figure S3). The use of the fluorescent protein allowed the position of the protein on the ssDNA to be correlated with the fluorescence state. This is more sensitive than using labels at the end of the DNA (21), whereby signals are only measured on interaction with the helicase. It also allowed simple changes to the DNA substrate.

This signal was then used to monitor PcrA translocation to the 5′-end of ssDNA, driven by ATP hydrolysis (Figure 2A). MDCC-PcrA was pre-mixed with different lengths of oligo(dT), rapidly mixed with ATP and then the fluorescence was followed with time. In all cases, the fluorescence decreased as PcrA translocated from an initial random binding along the ssDNA to the 5′-end (21). The decrease is completed when all PcrA molecules have reached that end, including those initially bound at or near the 3′-end. The time taken to reach the final fluorescence level, therefore, reports the translocation time for PcrA to move along the full length of the template. The duration of the fluorescence change increased linearly with ssDNA

length, and a plot of translocation time against ssDNA template length gives the translocation rate ([Figure 2]B). To validate the method, the rate was measured under the solution conditions used previously at $20°C$ ([21]) and gave a similar rate [99 (± 6) bases s^{-1}] here compared with 80 bases s^{-1}. The rate was also measured under the solution conditions used for plasmid unwinding in solution at $30°C$ ([14]) [244 (± 4) bases s^{-1}] and conditions similar to that used in the single-molecule unwinding assays at $23°C$ [133 (± 5) bases s^{-1}]. In all cases, the ssDNA translocation rate was significantly higher than values measured for PcrA-RepD moving along and unwinding dsDNA.

This method was exploited further to determine whether base composition affected the rate of ssDNA translocation ([Supplementary Figure S4]). Oligonucleotides with a single base type were compared ([Supplementary Figure S4A]). Oligo(dA) reached a minimum at a similar time to oligo (dT), whereas oligo (dC) was considerably faster. A mixed sequence of the same length showed a decrease in fluorescence with a similar end time to oligo(dA) and oligo(dT), but without a precise endpoint. The length dependence of the endpoints ([Supplementary Figure S4B]) gave 277 (± 15) bases s^{-1} and 526 (± 26) bases s^{-1} for the translocation rates on oligo(dA) and oligo(dC), respectively.

PcrA activity on immobilized, linear, biotinylated dsDNA using TIRFM

Unwinding activity of wild-type PcrA was measured using biotinylated linear dsDNA that had been immobilized on a microscope coverslip surface. dsDNA substrates from 500 to 1500 bp in length, tagged with a single-biotin label at the 5'-end of one strand and containing the *ori*D sequence near the other end, were immobilized on a streptavidin-coated coverslip. This approach closely mimics the bulk measurements (as described earlier in the text) because the helicase is distal from the coverslip surface and binds the dsDNA while in solution. Also, in principle, this experimental geometry allows loading of multiple helicases from solution or monomer exchange, as might occur in bulk experiments. The immobilized dsDNA templates were pre-incubated with RepD, enabling PcrA to load and unwind the RepD–DNA complex. The time course of unwinding was monitored by measuring the accumulation of Cy3B-SSB on the growing ssDNA strands ([Figure 3]). Fluorescent spots that increased in intensity to a maximum value were observed as the dsDNA was unwound. In the majority of events, a short-lived maximum plateau was observed, followed by either a single-step intensity drop to baseline or a stepwise decrease to half maximum intensity followed by a subsequent fall to baseline ([Figure 3]B and [Supplementary Table S1]). The rationale for the decrease is shown in [Supplementary Figure S5] in terms of stepwise dissociation of the two strands of ssDNA. The time course of the intensity rise for each unwinding event was characterized by two parameters, total increase in intensity (ΔI_{tot}) and total duration of unwinding (Δt_{tot}) ([Figure 3]). The distribution of these parameters provided information about the helicase processivity and the heterogeneity of its activity.

In the absence of RepD, the frequency of fluorescent spots that might be identified as unwinding events was very low ([Table 1]). This was consistent with the observation that PcrA in the absence of RepD had very low activity when measured in bulk assays of plasmid unwinding ([14]).

In the presence of RepD, many unwinding events were observed for all dsDNA template lengths ([Table 1]). The mean value of both Δt_{tot} and ΔI_{tot} ([Figures 4]A–C and [5]A–C) showed a linear dependence with the dsDNA length ([Figure 6]A), indicating complete unwinding of the dsDNA templates up to the length that is likely to remain in the evanescent field ([27]). A linear fit to the plot of mean Δt_{tot} versus dsDNA template length gave an unwinding rate of 31 (± 7) bp s^{-1}, in good agreement with the stopped-flow measurement (30 bp s^{-1}).

Event durations, Δt_{tot} ([Figure 4]A–C), and intensity changes, ΔI_{tot} ([Figure 5]A–C), were broadly distributed giving a wide range of estimated PcrA unwinding rates from 10 to 100 bp s^{-1}, whereas the unwinding speed measured for any one individual event occurred at a fairly constant rate. However, there was no correlation between individual Δt_{tot} and ΔI_{tot} values ([Supplementary Figure S6A]); hence, brief events could not simply be explained by premature termination of unwinding.

Individual traces were specifically examined for intermittent pausing during unwinding, as observed in earlier experiments using AddAB helicase ([27]). A 'pause' is defined here as a period of time with no increase in fluorescence intensity, which may result from stalling, back-stepping or dissociation of the helicase. The majority of events (>80%) showed no detectable pauses during unwinding. However, because the resolution of the assay is determined by the length of ssDNA that binds a single-SSB tetramer, ~ 65 bp in these assay conditions ([40]), equivalent to about 2 s of unwinding activity, we cannot exclude the possibility that there are shorter pauses.

To explore the potential effect of multiple PcrA molecules binding the dsDNA template simultaneously and/or exchange of PcrA between the solution and the DNA template, experiments were performed doubling the concentration of helicase (1000 nM). Although the average amplitude of the fluorescence intensity change remained unaffected ([Table 1] and [Supplementary Figure S7]), the unwinding duration was reduced by ~ 25%.

Activity of surface-immobilized bioPcrA on linear dsDNA using TIRFM

To study the processive unwinding activity of monomeric helicase molecules, an alternative experimental geometry was used in which biotinylated PcrA (bioPcrA) was bound to the surface of a streptavidin-coated microscope coverslip at limiting surface density. In control experiments, the bulk concentration of Cy3B-bioPcrA was systematically varied, and the number of fluorescent spots (corresponding to individual helicase molecules) per unit area was counted. There was a linear relationship between the number of spots and the bulk concentration of helicase up to 1 nM, which gave ~ 1 spot μm^{-2}. In addition for Cy3B-bioPcrA loading concentrations of ≤ 0.2 nM,
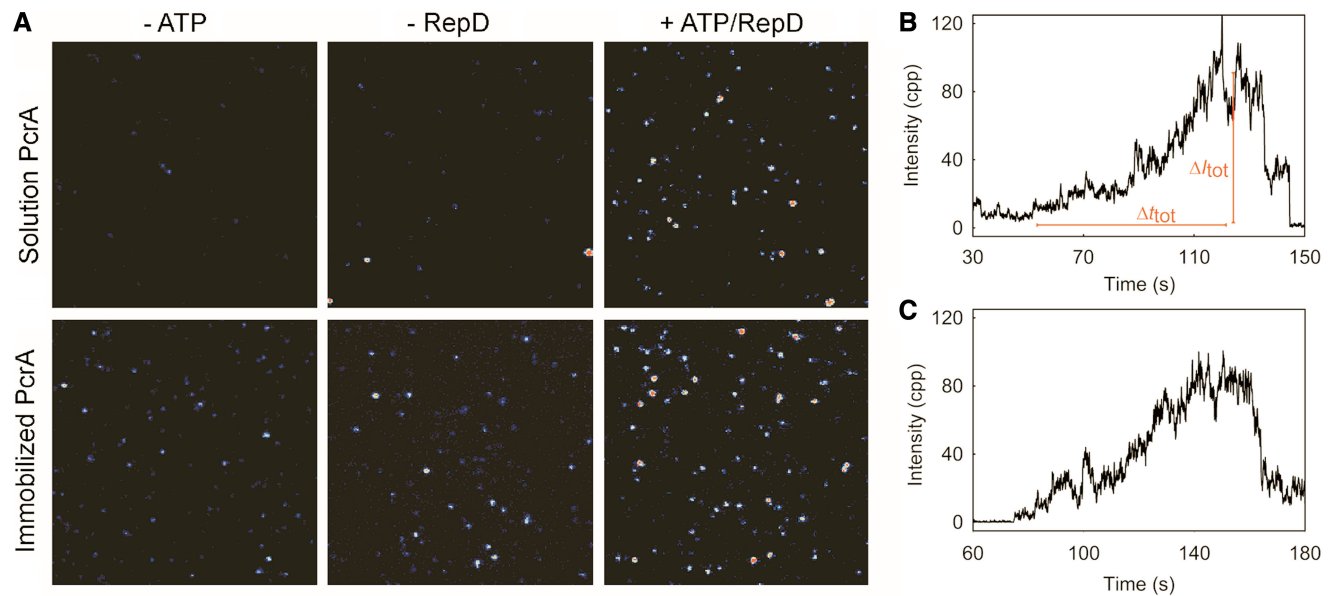
Figure 3. Visualization and analysis of 1-kb linear DNA unwinding by TIRFM. (**A**) Images of the microscope field showing the occurrence of fluorescent spots. Data are shown with and without ATP, and RepD, for solution and immobilized bioPcrA. Discrete fluorescent spots of increasing intensity appeared as individual DNA molecules were being progressively unwound. Representative intensity time courses are shown for solution (**B**) and immobilized bioPcrA (**C**). The two parameters used to define unwinding: the total event duration (Δt_{tot}) and the total increase in intensity (ΔI_{tot}) are shown here.

Table 1. Summary of helicase activity on immobilized linear DNA

[PcrA] (nM)	DNA length (bases)	Number of events	Mean duration ($\Delta t_{\text{tot}} \pm$ SEM) (s)	Mean intensity change ($\Delta I_{\text{tot}} \pm$ SEM) (cpp)	Rate ($\pm$ SEM) (bp s^{-1})
500	1500	159	47.8 (± 2.4)	63.4 (± 1.7)	31 (± 2)
500	1000	282	37.1 (± 1.1)	53.9 (± 1.1)	27 (± 1)
500	500	170	16.2 (± 0.9)	27.5 (± 0.7)	31 (± 2)
No RepD	1000	11			
1000	1000	162	28.7 (± 1.2)	51.9 (± 1.2)	35 (± 1)

Biotinylated linear dsDNA fragments containing the *ori*D sequence were immobilized on the PEGylated surface and incubated with RepD. Wild-type PcrA helicase, in the presence of Cy3B-SSB, was added. Helicase activity was initiated with 1 mM ATP. The events were defined by two parameters from the time course: the total event duration (Δt_{tot}) and the total increase in intensity (ΔI_{tot}). The unwinding rate stated here is calculated assuming complete unwinding of the DNA substrate during the duration of the event.

>90% of the spots had only single-photobleaching step. These data suggest that the large majority of fluorescent spots corresponded to a single-Cy3B-bioPcrA monomer. During the unwinding experiments (see later in the text), the density of unwinding events was between 0.15 and 0.2 μm^{-2}, which was sufficiently high to observe multiple unwinding events within a single-microscope field of view (50 $\times$ 50 μm^2) but low enough to ensure the observed events were due to a single-PcrA molecule (see Supplementary Methods and Supplementary Figure S8).

Linear dsDNA substrates, containing the *ori*D sequence at one end, were pre-incubated with RepD and then added to the immobilized helicase. Unwinding was initiated and analyzed as with the immobilized dsDNA (Figures 3–5). In the absence of ATP, no spots of increasing intensity were detected, rather, only a few spots of constant intensity were observed (Figure 3). Furthermore, in the absence of RepD, the frequency of unwinding events was very low, consistent with bulk assays that showed low activity of PcrA in the absence of RepD. However, in the presence of RepD and ATP, a large number of unwinding events were observed. Spot intensity changes during unwinding were characterized by a linear rise in intensity, followed by a plateau phase and then either a single- or two-step decrease in intensity back to baseline level, qualitatively similar to the situation with immobilized DNA. The distribution of stepwise drops in fluorescence is shown in Supplementary Table S1. Durations of the unwinding phase were linearly related to dsDNA template length, giving an unwinding rate of 44 bp s^{-1}, that is slightly faster than rates measured using the immobilized dsDNA geometry (Table 1 and 2 and Figures 3–6). Importantly, the intensity changes obtained with immobilized bioPcrA (Figure 5) were similar to those observed with solution PcrA. As with measurements using immobilized dsDNA, the distribution of unwinding durations with immobilized bioPcrA was broad (Figure 4), and there was no correlation between the

amplitude of spot intensity changes and the duration of unwinding (Supplementary Figure S6B).

To assess the ATP dependence of PcrA activity, the assay was repeated at 10 and 5 μM ATP for a 1-kb length of dsDNA (Table 2 and Supplementary Figure S9). These ATP concentrations bracket the K_m of 8 μM found from steady-state ATPase measurements (14). Experiments were performed as earlier in the text, but using time-lapse imaging to monitor the slower unwinding events. At 10 μM ATP, there was a 2-fold increase in the

unwinding duration relative to saturating ATP (1 mM), whereas at 5 μM, the duration increased $\sim$5-fold. Importantly, the ΔI_{tot} distributions were similar to those measured at saturating ATP, indicating full unwinding of the 1-kb dsDNA template at all ATP concentrations. The calculated unwinding rate decreased from 39 to 21 bp s^{-1} and 8 bp s^{-1} at 1 mM, 10 μM and 5 μM ATP, respectively (Table 2). The traces were also analyzed for pausing behavior during the unwinding phase, as described earlier in the text. At saturating ATP (1 mM), no pauses
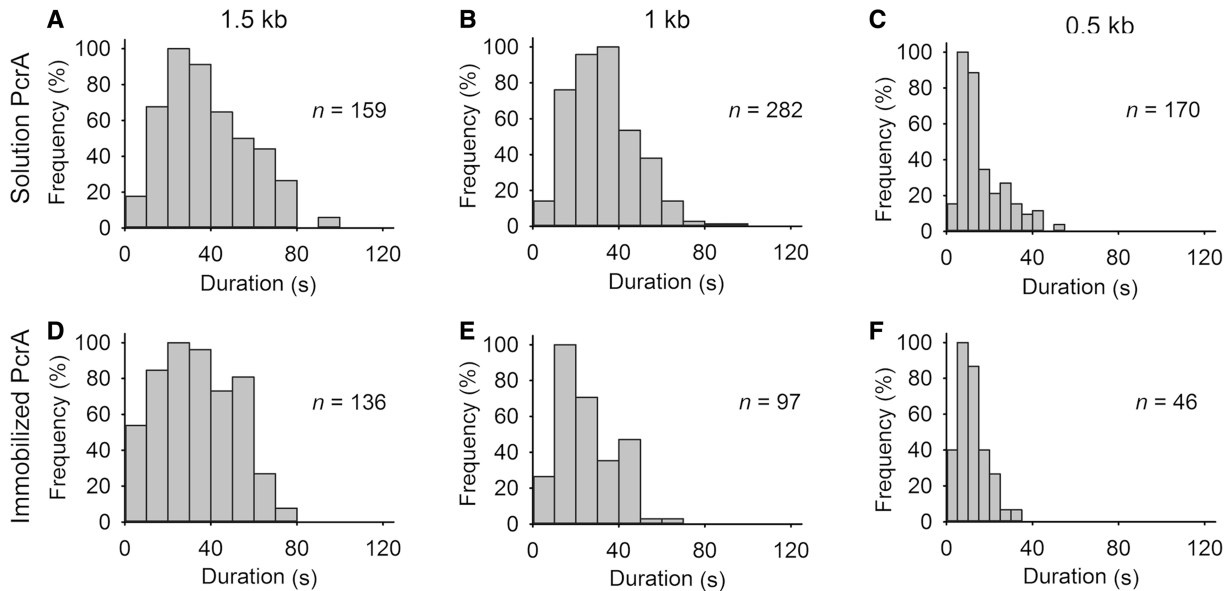
Figure 4. Distribution of durations of unwinding events for solution and immobilized bioPcrA with linear DNA. (**A–C**) Solution PcrA and (**D–F**) immobilized bioPcrA with the stated DNA lengths. The distributions of Δt_{tot} are presented as percentage frequency, normalized to the maximum.
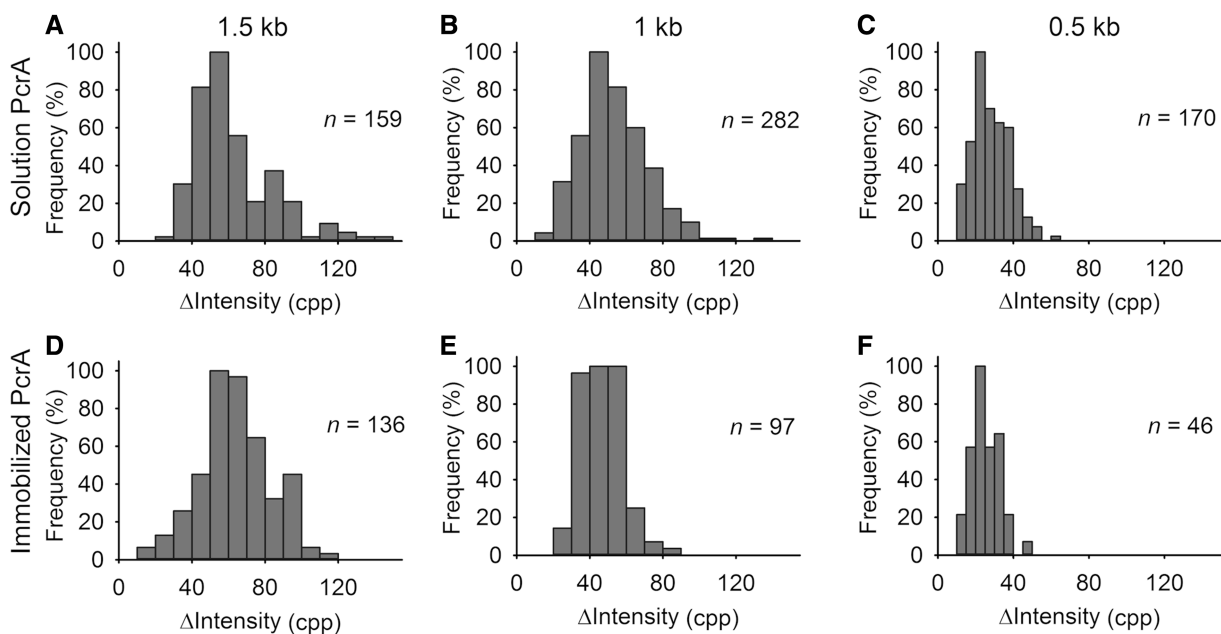
Figure 5. Distribution of intensity change for unwinding events with linear DNA. (**A–C**) solution PcrA and (**D–F**) immobilized bioPcrA with the stated DNA lengths. The distributions of ΔI_{tot} are presented as percentage frequency, normalized to the maximum.

could be detected. However, up to 40% of traces exhibited at least one significant pause at limiting ATP concentrations (i.e. $<10\,\mu M$).

The decrease in rate as ATP concentration is reduced confirms that the signal in this assay requires ATP hydrolysis. In the absence of ATP, fluorescent spots are constant (data not shown). This agrees with the observation from bulk assays that rapid ATP hydrolysis correlates with the fluorescent SSB signal (14).
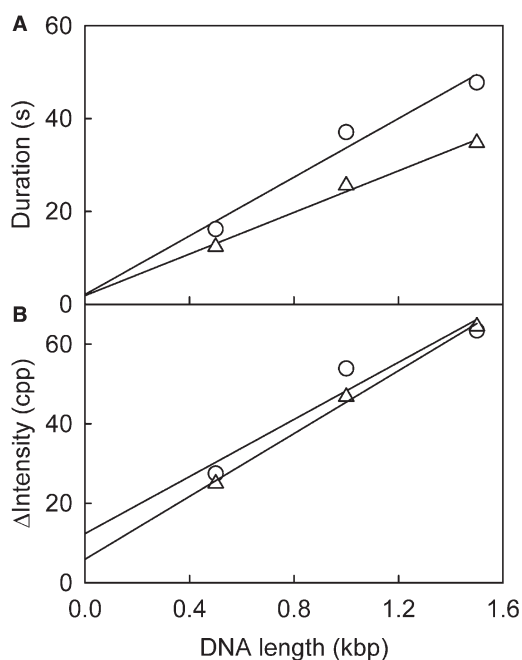
Figure 6. Dependence of mean unwinding durations and intensity changes on length of linear DNA. The unwinding durations (**A**) and intensity changes (**B**) are shown for various DNA lengths for solution PcrA (circles) and immobilized PcrA (squares). The best fit lines gave unwinding rates of 31 (± 7) $bp\,s^{-1}$ for solution PcrA and 44 (± 5) $bp\,s^{-1}$ for immobilized PcrA.

Activity of surface-immobilized bioPcrA on plasmid DNA using TIRFM

To approximate the conditions of PcrA activity *in vivo* more closely, unwinding assays were conducted with intact plasmids using surface-immobilized Cy3B-bioPcrA. Initial measurements using TIRFM showed there was a much shorter delay before the onset of unwinding ($3.9 \pm 0.1\,s$) than with artificial linear dsDNA templates. Therefore, to aid measurement, fluorescent Cy3B-bioPcrA was used to define the focal plane and identify the position of individual helicase molecules before unwinding was initiated by ATP addition. Cy3B-bioPcrA had the same maximum unwinding rate as unlabeled bioPcrA (see later in the text).

By loading RepD-nicked, 3094-bp plasmid, and then adding Cy3B-SSB and ATP, spots of increasing intensity were observed (Figure 7A and B). As with linear dsDNA, there were many such events in the field of observation, and these gave a broad range of durations and intensity increases (Figure 7C and D). Data from the set of measurements in Figure 7 are summarized in Table 2.

Assuming complete unwinding, the rate with Cy3B-bioPcrA is $37\,bp\,s^{-1}$ on the 3094-bp plasmid and measurement with unlabeled bioPcrA was similar with a rate of $40\,bp\,s^{-1}$. Measurements performed with a shorter 2437-bp plasmid (Supplementary Figure S10A–C and Table 2) gave a lower final intensity but a similar unwinding rate of $44\,bp\,s^{-1}$. In all experiments, there was a broad distribution of unwinding durations and peak intensity values, but very short events showed a correlation between duration and intensity (Supplementary Figure S10D), which will be discussed later in the text. As with linear DNA, stepwise drops in fluorescence were observed subsequent to unwinding with distribution shown in Supplementary Table S1. Such drops were ascribed to dissociation of the ssDNA from the complex, as in Supplementary Figure S5.

Table 2. Summary of helicase activity with immobilized bioPcrA

Linear or plasmid DNA	DNA length (bp)	ATP (μM)	Number of events	Mean duration ($\Delta t_{tot} \pm$ SEM) (s)	Mean intensity change ($\Delta I_{tot} \pm$ SEM) (cpp)	Rate ($\pm$SEM) ($bp\,s^{-1}$)
Linear	1500	1000	136	34.8 (± 1.7)	64.5 (± 4.4)	43 (± 2)
Linear	500	1000	40	12.4 (± 1.2)	25.0 (± 1.1)	40 (± 5)
Linear	1000	1000	97	25.6 (± 1.4)	46.8 (± 1.1)	39 (± 2)
Linear	1000	10	54	48.1 (± 3.6)	43.8 (± 2.5)	21 (± 2)
Linear	1000	5	73	131.5 (± 8.6)	46.3 (± 1.6)	8 (± 1)
Plasmid[a,b]	3094	1000	414	83.1 (± 2.0)	231.3 (± 5.6)	37 (± 2)
Plasmid[a]	2437	1000	333	55.5 (± 1.5)	217.9 (± 6.9)	44 (± 1)
Plasmid	3094	1000	211	77.6 (± 3.8)	114.1 (± 5.4)	40 (± 2)

BioPcrA was immobilized on the PEGylated surface. dsDNA fragments or plasmids containing the *oriD* sequence were incubated with RepD, before being incubated with bioPcrA surface. Helicase activity was initiated with ATP. The events were defined by two parameters from the time course: the total event duration (Δt_{tot}) and the total increase in intensity (ΔI_{tot}). The unwinding rate stated here is calculated assuming complete unwinding of the DNA substrate during the duration of the event. Intensity changes are not directly comparable between different sets of data because of different instrument configurations to optimize the signal in each case.
[a]Data were obtained with Cy3B-bioPcrA.
[b]Data were also analyzed by fitting a normal distribution and by determining the median values. A normal distribution gave a mean duration of 76.3 (± 2.4) s and a mean intensity change of 203.9 (± 1.1) cpp, giving a rate of 41 (± 1) $bp\,s^{-1}$. The median values were 75 s and 203 cpp, giving a rate of 41 $bp\,s^{-1}$.
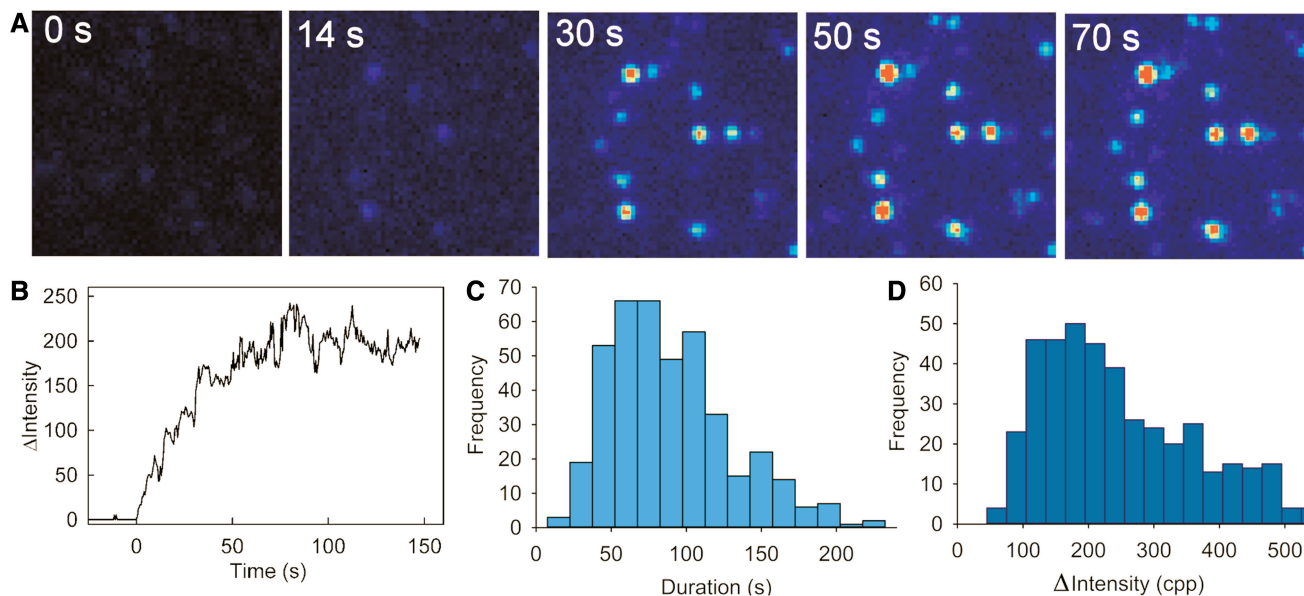
Figure 7. Visualization of circular plasmid DNA unwinding using immobilized PcrA. Cy3B-bioPcrA was used together with RepD and 3094-bp plasmid; see 'Material and Methods' section for details. Zero time was set as the time of the start of the unwinding event. (**A**) Visualization of individual fluorescent spots of increasing intensity with time on an area of $25\,\mu m^2$. (**B**) Representative example of time course. (**C**) Distribution of event durations for one experiment (414 events). The average duration is 83 (± 2) s, giving a rate of unwinding of 41 (± 1) s^{-1} for this set of events, assuming complete unwinding. (**D**) Distribution of event intensity changes. The data from this set of measurements are summarized in Table 2.

DISCUSSION

The ssDNA translocation and dsDNA unwinding rates of PcrA helicase were measured using a combination of bulk solution and single-molecule TIRF-based assays. In the TIRF assays, individual PcrA·RepD–dsDNA complexes were immobilized on a microscope coverslip either via the helicase or the dsDNA (Figures 3 and 7). In both geometries, unwinding was measured by the rate of accumulation of fluorescent Cy3B-SSB to the nascent ssDNA. The time course of unwinding was compared using different dsDNA templates, concentrations of PcrA and ATP and in the presence and absence of the initiation partner, RepD (summarized in Table 3).

An advantage of this TIRFM assay is that many unwinding events could be recorded simultaneously within the field of view. Furthermore, the activity of single complexes of PcrA with RepD in the presence of SSB more closely mimics the conditions *in vivo* than equivalent experiments on the helicase in isolation. The approach is, therefore, suitable to address a variety of questions about processivity, heterogeneity of unwinding and oligomeric state of PcrA under near physiological conditions.

Active oligomeric state and processivity of PcrA

There has been debate about the oligomeric state of various helicases, including PcrA (22). In that earlier study, it was proposed that more than one PcrA molecule might be required to hold the leading monomer in place, stabilizing its interactions with the DNA substrate. However, kinetic studies and crystal structures have been unable to provide a definitive

Table 3. Summary of unwinding and translocation rates

Measurement[a]	PcrA	DNA	Rate (bases s^{-1})
Stopped flow	Solution	Plasmid	27
TIRFM	Solution	Linear (Bio-DNA)	31
TIRFM	BioPcrA	Linear	44
TIRFM	BioPcrA	Plasmid	42
Stopped flow (translocation)	Solution (MDCC-PcrA)	ssDNA [Oligo(dT)]	133

Measurements were for the same solution conditions (50 mM Tris–HCl, pH 7.5, 100 mM KCl, 10 mM MgCl$_2$ and 1 mM EDTA, 22°C–24°C). Rates are for fits to durations for different lengths of DNA (Figures 2 and 6, Supplementary Figure S2), except for plasmid unwinding, for which the length range was small; therefore, the rate is the average of two lengths, calculated assuming complete unwinding: details are given in the text.
[a]Unwinding dsDNA containing *ori*D in the presence of RepD, except as indicated.

answer regarding the active, oligomeric state of PcrA in the presence of RepD and SSB.

Characterization of PcrA in terms of oligomerization was addressed with immobilized bioPcrA. SEC-MALS (Supplementary Figure S1) shows that PcrA and bioPcrA are monomeric in solution under both single-molecule and bulk assay conditions, consistent with previously reported gel filtration measurements (35). To ensure it was monomeric during the unwinding assays, bioPcrA was immobilized at low-surface density in the absence of DNA, so that premature dissociation would result in loss of the DNA from the surface. Sudden disappearance of the fluorescence spot would be identified as

short-lived low-intensity events. With linear dsDNA, such events were rare and did not show up in correlation plots of intensity and. duration (Supplementary Figure S6). The single-molecule assays using immobilized bioPcrA, with both linear and circular (plasmid) dsDNA–RepD complexes, show that a single-PcrA monomer is sufficient for processive DNA unwinding. Although, in principle, conditions in the cell might allow multiple PcrA molecules to bind behind the unwinding junction, as proposed for some other helicases (23,41), the presence of both polymerase and SSB make this much less likely and support the idea of a single-monomeric PcrA being the functional unit *in vivo*.

For plasmid replication to be conducted rapidly and completely *in vivo*, replicative helicases, such as PcrA, are likely to be highly processive enzymes. Both of our single-molecule geometries, when either the dsDNA or the bioPcrA is surface-immobilized, show that monomeric PcrA is able to completely unwind up to 3 kb of RepD–dsDNA.

Several lines of evidence for high processivity from this work are now discussed in more detail. Results obtained using both helicase and linear dsDNA immobilization strategies showed that the durations of unwinding and peak intensity changes were linearly dependent on DNA length (Figure 6), suggesting complete unwinding. Furthermore, the unwinding speed was similar for both experimental formats and in good agreement with data obtained using stopped-flow analysis in bulk solution. The maximum intensity values measured in an earlier study, under identical conditions, using the highly processive AddAB helicase (27) were similar to those reported here. Finally, the fact that the fluorescence signal plateaus can fall to background level in two equal steps at the end of unwinding (Supplementary Table S1) is again evidence for complete unwinding. Observation of either one or two stepwise decreases in intensity back to the baseline level is explained by either simultaneous or sequential release of the two product ssDNA strands (Supplementary Figure S5). It is difficult to envision a partly unwound dsDNA template behaving like this unless PcrA has DNA nuclease activity, for which there is no experimental evidence.

Plasmid unwinding

We believe this is the first time that helicase activity has been observed at the single-molecule level on a native plasmid substrate. Most single-molecule approaches are limited to working with linear dsDNA substrates, whereas the current method enables study of intact circular plasmids, ~3000-bp long (Figure 7 and Supplementary Figure S10). Our previous work, with AddAB helicase, showed that linear dsDNA templates up to 1500 bp in length remained within in the evanescent field when unwound to ssDNA and bound with Cy3B-SSB (27). A shorter, 2400-bp, plasmid gave a reduction in final fluorescence amplitude, proportional to the reduced number of bound Cy3B-SSB.

Bacterial plasmids are initially supercoiled, leading to more efficient nicking by RepD than with linear DNA (16,42); hence, a greater proportion of the plasmid DNA

was likely to be unwound as was observed in solution (14). Qualitatively this was reflected in the higher density of unwinding events observed in the TIRFM. The unwinding rate (42 bp s^{-1}) found for bioPcrA acting on circular plasmid DNA was similar to that measured with linear dsDNA templates (44 bp s^{-1}) (Table 3). The most important finding is that the 3094-bp circular plasmid could be fully unwound by a single bioPcrA in the presence of the initiator protein RepD.

However, short events showed correlation with intensity (Supplementary Figure S10) and analysis of these (~10% of total events Supplementary Table S1), showed a high proportion that did not show a drop in fluorescence subsequent to unwinding, suggesting stalling was the major reason for the short time events and low fluorescence. Such stalling could be due to the DNA becoming stuck on the surface. Although this is a small fraction of all events, the data for this plasmid were analyzed in three ways to get an 'average' unwinding rate (Table 2), namely, obtaining the mean, the median and a fitting a normal distribution. The three unwinding rates obtained were similar, suggesting that the small population of stalled events does not affect the value significantly.

Pausing and heterogeneity of unwinding rates

We now consider how the variation in unwinding rates may be affected by the detailed mechanism. PcrA in solution has a similar average unwinding rate both in single-molecule (31 bp s^{-1}) and bulk assays (30 bp s^{-1}) (Table 3). The rate is slightly higher, if bioPcrA is immobilized for both linear (44 bp s^{-1}) and plasmid DNA (42 bp s^{-1}). This is not because of the bioPcrA modifications (labeling or biotinylation), as these variants behave like wild-type PcrA in bulk unwinding assays.

It is possible that these variations in rate are due to a small fraction of complexes pausing briefly when PcrA is in solution. In contrast to the situation with immobilized PcrA, premature dissociation of solution PcrA would not lead to loss of a fluorescent spot and might well result in a short pause followed by re-association of a new PcrA to continue unwinding. This might be explained if the nucleotide-free state of PcrA binds less tightly to DNA, and so it occasionally dissociates before ATP binds. This effect might lead to longer unwinding times with PcrA in solution.

In addition to this variation in average rate, unwinding of individual helicase complexes were heterogeneous with rates ranging from ~10 to 100 bp s^{-1} (Figure 4). If this were due to incomplete unwinding, short events would have a low intensity, and long events would have a high intensity. However, with linear DNA, there was no correlation between the amplitude of the fluorescence signal and the duration of the event. As described earlier in the text, such correlation does occur with the shortest ~10% of events with plasmid DNA, typically twice as long as the linear substrates used.

At saturating ATP concentrations (1 mM), a small fraction of unwinding events (<20%) with immobilized linear DNA, exhibited at least one observable pause

(>2 s duration), but this was insufficient to explain the large heterogeneity in individual unwinding rates. The possibility of PcrA dissociation and re-association was tested by doubling the solution concentration of PcrA. The frequency of long-lived unwinding events was greatly reduced but not eliminated (Supplementary Figure S7), presumably because of more rapid rebinding of PcrA at higher concentrations. A more likely explanation of the wide rate dispersion is that the nascent ssDNA either becomes tangled or the Cy3B-SSB fails to pack optimally along the ssDNA chains, perhaps allowing base pairing to occur in some regions of two nascent DNA strands. Alternatively, particular regions of secondary structure or DNA damage could contribute to the range of observed rates. *In vivo* the presence of DNA polymerase III would prevent base pairing of the evolved single-strand because the complementary strand would be duplex DNA.

Interaction with initiator protein RepD?

Our data are consistent with the proposal, based on structural studies (18), that monomeric PcrA coupled to RepD is the functional helicase. With immobilized DNA in the absence of RepD, few events were observed, consistent with PcrA on its own being a poor helicase (11,12) and RepD being required for helicase activity. This highlights the importance of partner proteins in regulating helicase activity, given that an unregulated helicase could be deleterious to the cell. Furthermore, many helicases, including PcrA, have multiple cellular functions, which consist of translocase and helicase activities, whereby binding partners can act as important switches between these modes. The changes in motor activity observed between these two modes are discussed later in the text. Although the interaction interface between PcrA and RepD remains to be defined, it is tempting to speculate that RepD may bind to the PcrA 2B domain thereby alleviating an autoinhibitory effect on the helicase (43). Alternatively, RepD might stabilize the interaction between PcrA and the DNA by forming a channel through which the duplex DNA has to pass. In support of this idea, it has been shown that RepD does not greatly affect the motor activity of PcrA in terms of the ATPase cycle (44), but it increases its affinity for DNA (14).

Evidence for an interaction could be obtained from the intensity traces (Figure 3), in which a plateau was observed at the end of unwinding and can be followed by a two-step decrease in intensity (Figure 3 and Supplementary Table S1). Direct interaction of PcrA and RepD could hold together both DNA strands briefly at the end of unwinding, before the stepwise release of the ssDNA products. Such a plateau was a frequent feature of unwinding events.

Rate of dsDNA unwinding compared with ssDNA translocation and their ATP usage

The rate of plasmid unwinding measured in bulk and TIRFM assays by PcrA and RepD was compared with measuring the translocation rate of PcrA on ssDNA, as summarized in Table 3. PcrA alone is essentially unable to unwind significant lengths of dsDNA in the absence of the

initiator protein (here RepD) (11,12); therefore, a direct comparison of the translocation and unwinding of either the PcrA-RepD complex or PcrA alone was not possible. However, it is still possible to assess how the nature of dsDNA unwinding, or the effect of RepD, perturb the motor activity of PcrA.

Plasmid unwinding occurs at $\sim$42 bp s^{-1}, (average for the two lengths), similar to the rate of unwinding with linear dsDNA and immobilized PcrA. Unwinding in solution gives 27 bp s^{-1} (Supplementary Figure S2). However, under the same conditions, translocation along ssDNA occurs at 133 bases s^{-1} (Table 3, Figure 2), much faster than it unwinds dsDNA. The precise rate of ssDNA translocation depends on the base content of the DNA (Supplementary Figure S4), suggesting movement of the bases among the base binding pockets of PcrA limits the observed rate.

Interestingly, the single-molecule assays show that some helicase complexes can also reach relatively fast rates of 100 bp s^{-1}, perhaps limited by the translocation rate. One explanation is that PcrA unwinds dsDNA by a mechanism that is partly passive in character.

The coupling between the ATP hydrolysis reaction and PcrA base translocation is one ATP per base both for ssDNA translocation and for dsDNA unwinding (14,20), even though the two rates of movement are different. A structural basis for 1:1 coupling was first suggested from structural analysis for ssDNA movement (45). A passive mechanism presents the danger of futile hydrolysis, uncoupled from movement during dsDNA unwinding. However, because the coupling remains tight (1 base per ATP), such futile ATP hydrolysis does not occur here, even during the slower dsDNA unwinding. This can be rationalized by the ATP cleavage step itself being closely coupled to single-base movement during each ATPase cycle. Any delay in movement, such as awaiting the spontaneous separation of base pairs in the DNA, as proposed for a passive mechanism, would also delay the cleavage step. That is, no ATP cleavage can occur except during movement. Such an interpretation is fully consistent with the structural changes that occur between the ATP and ADP states (17,18,45–48). It is also consistent with the fact that the cleavage step is the main process greatly accelerated by interaction with DNA, but it is rate limiting in the ATPase cycle for both ssDNA and dsDNA movement, followed by rapid phosphate release (44).

In summary, we have performed a detailed, kinetic analysis of PcrA helicase activity using bulk solution and single-molecule approaches with ssDNA, linear dsDNA and plasmid DNA. We have determined that an individual monomeric PcrA helicase, in combination with RepD, has a high processivity enabling $\sim$3000-bp plasmid lengths of dsDNA to be unwound. We give evidence for a direct interaction between PcrA and RepD, which may explain that, although RepD enhances helicase activity, it may be able to perturb the motor activity of PcrA. The assay provides a basis for reconstituting the entire replication machinery so that rolling-circle plasmid replication can be followed in real-time at the single-molecule level.

SUPPLEMENTARY DATA

Supplementary Data are available at NAR Online: Supplementary Table 1, Supplementary Figures 1–10 and Supplementary Method.

REFERENCES

1. Gorbalenya,A.E. and Koonin,E.V. (1993) Helicases: amino acid sequence comparisons and structure-function relationships. *Curr. Opin. Struct. Biol.*, **3**, 419–429.
2. Singleton,M.R., Dillingham,M.S. and Wigley,D.B. (2007) Structure and mechanism of helicases and nucleic acid translocases. *Annu. Rev. Biochem.*, **76**, 23–50.
3. Atkinson,J., Gupta,M.K. and McGlynn,P. (2011) Interaction of Rep and DnaB on DNA. *Nucleic Acids Res.*, **39**, 1351–1359.
4. Chao,K.L. and Lohman,T.M. (1991) DNA-induced dimerization of the *Escherichia coli* Rep helicase. *J. Mol. Biol.*, **221**, 1165–1181.
5. Arthur,H.M. and Lloyd,R.G. (1980) Hyper-recombination in *uvr*D mutants of *Escherichia coli* K-12. *Mol. Gen. Gen.*, **180**, 185–191.
6. Veaute,X., Delmas,S., Selva,M., Jeusset,J., Le Cam,E., Matic,I., Fabre,F. and Petit,M.A. (2005) UvrD helicase, unlike Rep helicase, dismantles RecA nucleoprotein filaments in *Escherichia coli*. *EMBO J.*, **24**, 180–189.
7. Yamaguchi,M., Dao,V. and Modrich,P. (1998) MutS and MutL activate DNA helicase II in a mismatch-dependent manner. *J. Biol. Chem.*, **273**, 9197–9201.
8. Greenstein,D. and Horiuchi,K. (1987) Interaction between the replication origin and the initiator protein of the filamentous phage f1: binding occurs in two steps. *J. Mol. Biol.*, **197**, 157–174.
9. Yarranton,G.T. and Gefter,M.L. (1979) Enzyme-catalyzed DNA unwinding: studies on *Escherichia coli* rep protein. *Proc. Natl Acad. Sci. USA*, **76**, 1658–1662.
10. Iordanescu,S. and Bargonetti,J. (1989) *Staphylococcus aureus* chromosomal mutations that decrease efficiency of Rep utilization in replication of pT181 and related plasmids. *J. Bacteriol.*, **171**, 4501–4503.
11. Soultanas,P., Dillingham,M.S., Papadopoulos,F., Phillips,S.E., Thomas,C.D. and Wigley,D.B. (1999) Plasmid replication initiator protein RepD increases the processivity of PcrA DNA helicase. *Nucleic Acids Res.*, **27**, 1421–1428.
12. Niedziela-Majka,A., Chesnik,M.A., Tomko,E.J. and Lohman,T.M. (2007) *Bacillus stearothermophilus* PcrA monomer Is a single-stranded DNA translocase but not a processive helicase *in vitro*. *J. Biol. Chem.*, **282**, 27076–27085.
13. Zhang,W., Dillingham,M.S., Thomas,C.D., Allen,S., Roberts,C.J. and Soultanas,P. (2007) Directional loading and stimulation of PcrA helicase by the replication initiator protein RepD. *J. Mol. Biol.*, **371**, 336–348.
14. Slatter,A.F., Thomas,C.D. and Webb,M.R. (2009) PcrA helicase tightly couples ATP hydrolysis to unwinding double-stranded DNA, modulated by the replication initiator protein, RepD. *Biochemistry*, **48**, 6326–6334.
15. Noirot,P., Bargonetti,J. and Novick,R.P. (1990) Initiation of rolling-circle replication in pT181 plasmid: initiator protein enhances cruciform extrusion at the origin. *Proc. Natl Acad. Sci. USA.*, **87**, 8560–8564.
16. Arbore,C., Lewis,L.M. and Webb,M.R. (2012) Kinetic mechanism of initiation by RepD as a part of asymmetric, rolling circle plasmid unwinding. *Biochemistry*, **51**, 3684–3693.
17. Subramanya,H.S., Bird,L.E., Brannigan,J.A. and Wigley,D.B. (1996) Crystal structure of DExx box DNA helicase. *Nature*, **384**, 379–383.
18. Velankar,S.S., Soultanas,P., Dillingham,M.S., Subramanya,H.S. and Wigley,D.B. (1999) Crystal structures of complexes of PcrA DNA helicase with a DNA substrate indicate an inchworm mechanism. *Cell*, **97**, 75–84.
19. Dillingham,M.S., Soultanas,P., Wiley,P., Webb,M.R. and Wigley,D.B. (2001) Defining the roles of individual residues in the single-stranded DNA binding site of PcrA helicase. *Proc. Natl Acad. Sci. USA.*, **98**, 8381–8387.
20. Dillingham,M.S., Wigley,D.B. and Webb,M.R. (2000) Demonstration of unidirectional single-stranded DNA translocation by PcrA helicase: measurement of step size and translocation speed. *Biochemistry*, **39**, 205–212.
21. Dillingham,M.S., Wigley,D.B. and Webb,M.R. (2002) Direct measurement of single stranded DNA translocation by PcrA helicase using the fluorescent base analogue 2-aminopurine. *Biochemistry*, **41**, 643–651.
22. Yang,Y., Dou,S.X., Ren,H., Wang,P.Y., Zhang,X.D., Qian,M., Pan,B.Y. and Xi,X.G. (2008) Evidence for a functional dimeric form of the PcrA helicase in DNA unwinding. *Nucleic Acids Res.*, **36**, 1976–1989.
23. Byrd,A.K. and Raney,K.D. (2005) Increasing the length of the single-stranded overhang enhances unwinding of duplex DNA by bacteriophage T4 Dda helicase. *Biochemistry*, **44**, 12990–12997.
24. Manosas,M., Xi,X.G., Bensimon,D. and Croquette,V. (2010) Active and passive mechanisms of helicases. *Nucleic Acids Res.*, **38**, 5518–5526.
25. Lohman,T.M. (1992) *Escherichia coli* DNA helicases: mechanisms of DNA unwinding. *Mol. Microbiol.*, **6**, 5–14.
26. Byrd,A.K., Matlock,D.L., Bagchi,D., Aarattuthodiyil,S., Harrison,D., Croquette,V. and Raney,K.D. (2012) Dda helicase tightly couples translocation on single-stranded DNA to unwinding of duplex DNA: Dda Is an optimally active helicase. *J. Mol. Biol.*, **420**, 141–154.
27. Fili,N., Mashanov,G., Toseland,C.P., Batters,C., Wallace,M.I., Yeeles,J.T.P., Dillingham,M.S., Webb,M.R. and Molloy,J.E. (2010) Visualizing DNA unwinding by helicases at the single molecule level. *Nucleic Acids Res.*, **38**, 4448–4457.
28. Fili,N., Toseland,C.P., Dillingham,M.S., Webb,M.R. and Molloy,J.E. (2011) A single-molecule approach to visualize DNA unwinding. *Methods Mol. Biol.*, **778**, 193–214.
29. Yeeles,J.T.P., Gwynn,E.J., Webb,M.R. and Dillingham,M.S. (2011) The AddAB helicase-nuclease catalyses rapid and processive DNA unwinding using a single Superfamily 1A motor domain. *Nucleic Acids Res.*, **39**, 2271–2285.
30. Corrie,J.E.T. (1994) Thiol-reactive fluorescent probes for protein labelling. *J. Chem. Soc. Perkin Trans. I*, 2975–2982.
31. Dillingham,M.S., Tibbles,K.L., Hunter,J.L., Bell,J.C., Kowalczykowski,S.C. and Webb,M.R. (2008) Fluorescent single-stranded DNA binding protein as a probe for sensitive, real time assays of helicase activity. *Biophys. J.*, **95**, 3330–3339.
32. Kunzelmann,S., Morris,C., Chavda,A.P., Eccleston,J.F. and Webb,M.R. (2010) Mechanism of interaction between single-stranded DNA binding protein and DNA. *Biochemistry*, **49**, 843–852.
33. Brune,M., Hunter,J.L., Howell,S.A., Martin,S.R., Hazlett,T.L., Corrie,J.E.T. and Webb,M.R. (1998) Mechanism of inorganic phosphate interaction with phosphate binding protein from *Escherichia coli*. *Biochemistry*, **37**, 10370–10380.

34. Webb,M.R. (2003) A fluorescent sensor to assay inorganic phosphate. In: Johnson,K.A. (ed.), *Kinetic Analysis of Macromolecules: a Practical Approach*. Oxford University Press, Oxford, UK, pp. 131–152.

35. Bird,L.E., Brannigan,J.A., Subramanya,H.S. and Wigley,D.B. (1998) Characterisation of *Bacillus stearothermophilus* PcrA helicase: evidence against an active rolling mechanism. *Nucleic Acids Res.*, **26**, 2686–2693.

36. Thomas,C.D., Nikiforov,T.T., Connolly,B.A. and Shaw,W.V. (1995) Determination of sequence specificity between a plasmid replication initiator protein and the origin of replication. *J. Mol. Biol.*, **254**, 381–391.

37. Leatherbarrow,R.J. (2007) *GraFit Version 6*. Erithacus Software Ltd., Horley, UK.

38. Mashanov,G.I. and Molloy,J.E. (2007) Automatic detection of single fluorophores in live cells. *Biophys. J.*, **92**, 2199–2211.

39. Sellers,J.R. and Veigel,C. (2010) Direct observation of the myosin-Va power stroke and its reversal. *Nat. Struct. Mol. Biol.*, **17**, 590–595.

40. Lohman,T.M. and Ferrari,M.E. (1994) *Escherichia coli* single-stranded DNA-binding protein: multiple DNA-binding modes and cooperativities. *Annu. Rev. Biochem.*, **63**, 527–570.

41. Levin,M.K., Wang,Y.H. and Patel,S.S. (2004) The functional interaction of the hepatitis C virus helicase molecules is responsible for unwinding processivity. *J. Biol. Chem.*, **279**, 26005–26012.

42. Thomas,C.D., Balson,D.F. and Shaw,W.V. (1990) *In vitro* studies of the initiation of Staphylococcal plasmid replication. Specificity of RepD for its origin (*oriD*) and characterization of the RepD-*ori* tyrosyl ester intermediate. *J. Biol. Chem.*, **265**, 5519–5530.

43. Cheng,W., Brendza,K.M., Gauss,G.H., Korolev,S., Waksman,G. and Lohman,T.M. (2002) The 2B domain of the *Escherichia coli* Rep protein is not required for DNA helicase activity. *Proc. Natl Acad. Sci. USA*, **99**, 16006–16011.

44. Toseland,C.P., Martinez-Senac,M.M., Slatter,A.F. and Webb,M.R. (2009) The ATPase cycle of PcrA helicase and its coupling to translocation on DNA. *J. Mol. Biol.*, **392**, 1020–1032.

45. Soultanas,P., Dillingham,M., Wiley,P., Webb,M.R. and Wigley,D.B. (2000) Uncoupling DNA translocation and helicase activity in pcrA: direct evidence for an active mechanism. *EMBO J.*, **19**, 3799–3810.

46. Dillingham,M.S., Soultanas,P. and Wigley,D.B. (1999) Site-directed mutagenesis of motif III in PcrA helicase reveals a role in coupling ATP hydrolysis to strand separation. *Nucleic Acids Res.*, **27**, 3310–3317.

47. Soultanas,P. and Wigley,D.B. (2000) DNA helicases: 'inching forward'. *Curr. Opin. Struct. Biol.*, **10**, 124–128.

48. Lee,J.Y. and Yang,W. (2006) UvrD helicase unwinds DNA one base pair at a time by a two-part power stroke. *Cell*, **127**, 1349–1360.